

## The fundamental frequency of vibration of rectangular wood and plywood plates

This content has been downloaded from IOPscience. Please scroll down to see the full text.

1946 Proc. Phys. Soc. 58 78

(<http://iopscience.iop.org/0959-5309/58/1/307>)

View [the table of contents for this issue](#), or go to the [journal homepage](#) for more

Download details:

IP Address: 137.30.242.61

This content was downloaded on 27/06/2014 at 16:38

Please note that [terms and conditions apply](#).

# THE FUNDAMENTAL FREQUENCY OF VIBRATION OF RECTANGULAR WOOD AND PLYWOOD PLATES

By R. F. S. HEARMON,  
Princes Risborough

*Communicated by W. W. Barkas 24 September 1945*

**ABSTRACT.** Equations are derived expressing the frequency of vibration of rectangular wood and plywood plates in terms of elastic constants, dimensions and density. For supported edges, the solution is exact and gives the complete series of overtones. For clamped edges, the fundamental frequency is estimated by the approximate Rayleigh method, but evidence is presented which indicates that the errors introduced by the use of the Rayleigh method are, in fact, negligible. A method of measuring the frequencies is described; comparison of calculated with observed frequencies shows that the former are on the average about 23% high for clamped edges and about the same amount low for supported edges. This discrepancy is attributed to lack of correspondence between the experimental edge conditions and those assumed in the theoretical treatment. Finally, an empirical method, based on the rough proportionality between elastic constants and density of wood, is suggested and justified for obtaining approximate estimates of the fundamental frequencies in terms of plate dimensions only.

## INTRODUCTION

CONSIDERABLE advances have recently been made in the elastic theory of wood and plywood. This theory has been used to calculate stresses and deflections under lateral loading and critical buckling stresses of plywood plates; the agreement with experiment is reasonable though not exact. The frequency of vibration can be obtained theoretically by closely allied methods, and one of the objectives of the present investigation is to extend the comparison between theory and experiment to this frequency. A second objective is to gain some information regarding the frequency, which does not appear to have been studied hitherto.

### §1. DEFINITIONS AND BASIC EQUATIONS

As is usual in problems of this type, it is assumed that the material is homogeneous and perfectly elastic and that, in the two-dimensional case, its elastic behaviour is determined by the existence of two perpendicular symmetry axes. For the particular purpose of the present investigation, it is further assumed that the symmetry axes (i.e. the directions parallel and perpendicular to the grain) are parallel with the sides of the plate. The dimensions of the plate are  $a$ ,  $b$  and  $h$ , where

$a$  = length of side parallel with  $Ox$ .

$b$  = " " " " " "  $Oy$ .

$h$  = thickness of plate, parallel with  $Ox$ .

( $h$  is small in comparison with  $a$  and  $b$ .)

Under these conditions the differential equation governing the small deflections  $w$  in the  $Oz$  direction is (March, 1936, 1942)

$$D_1 \frac{\partial^4 w}{\partial x^4} + D_2 \frac{\partial^4 w}{\partial y^4} + 2D_3 \frac{\partial^4 w}{\partial x^2 \partial y^2} - P = 0, \quad \dots\dots (1.1)$$

where

$$\left. \begin{aligned} D_1 &= \frac{E_1 h^3}{12\lambda}; \\ D_2 &= \frac{E_2 h^3}{12\lambda}; \\ D_3 &= \frac{E_1 \sigma_{21} h^3}{12\lambda} + \frac{G_{12} h^3}{6} \\ &= D_4 + 2D_5; \end{aligned} \right\} \quad \dots\dots (1.2)$$

$E_1$  = Young's modulus in bending in  $Ox$  direction ;

$E_2$  = " " " " " "  $Oy$  " ;

$G_{12}$  = Rigidity modulus for shear stresses in  $Ox$  and  $Oy$  directions ;

$\sigma_{21} = \frac{\text{contraction in } Ox \text{ direction}}{\text{extension in } Oy \text{ direction}}$  for tension in  $Oy$  direction ;

$\lambda = 1 - \sigma_{21} \sigma_{12} \approx 0.99$  for wood and plywood ;

$P$  = pressure acting in  $Oz$  direction.

The differential equation governing the vibration of the plate can be found by substituting  $\rho h(\partial^2 w / \partial t^2)$  for  $-P$  in (1.1) :

$$D_1 \frac{\partial^4 w}{\partial x^4} + D_2 \frac{\partial^4 w}{\partial y^4} + 2D_3 \frac{\partial^4 w}{\partial x^2 \partial y^2} + \rho h \frac{\partial^2 w}{\partial t^2} = 0, \quad \dots\dots (1.3)$$

where  $\rho$  = density of material (weight at test/volume at test) and  $t$  = time.

The boundary conditions for a plate clamped at the edges are (Timoshenko, 1940, § 22) :

$$\left. \begin{aligned} w &= 0 \text{ at:—} & x=0, & x=a, & y=0, & y=b ; \\ \frac{\partial w}{\partial x} &= 0 \text{ at:—} & x=0, & x=a ; \\ \frac{\partial w}{\partial y} &= 0 \text{ at:—} & y=0, & y=b ; \end{aligned} \right\} \quad \dots\dots (1.4)$$

while for a plate simply supported at the edges they are (Timoshenko, 1940, §§ 22, 26) :

$$\left. \begin{aligned} w &= 0 \text{ at:—} & x=0, & x=a, & y=0, & y=b ; \\ \frac{\partial^2 w}{\partial x^2} &= 0 \text{ at:—} & x=0, & x=a ; \\ \frac{\partial^2 w}{\partial y^2} &= 0 \text{ at:—} & y=0, & y=b. \end{aligned} \right\} \quad \dots\dots (1.5)$$

The potential energy of bending ( $V$ ) is (March, 1942 ; Goland, 1942) :

$$V = \frac{1}{2} \int_0^a \int_0^b \left\{ D_1 \left( \frac{\partial^2 w}{\partial x^2} \right)^2 + D_2 \left( \frac{\partial^2 w}{\partial y^2} \right)^2 + 2D_4 \frac{\partial^2 w}{\partial x^2} \frac{\partial^2 w}{\partial y^2} + 4D_5 \left( \frac{\partial^2 w}{\partial x \partial y} \right)^2 \right\} dx dy, \quad \dots\dots(1.6)$$

and the kinetic energy  $T$  is

$$T = \frac{\rho h}{2} \int_0^a \int_0^b \left( \frac{\partial w}{\partial t} \right)^2 dx dy. \quad \dots\dots(1.7)$$

## § 2. DERIVATION OF THE FREQUENCY EQUATIONS

In the case of supported edges, an exact solution can be obtained by expressing  $w$  as

$$w = w_0 \sin \frac{m\pi x}{a} \sin \frac{n\pi y}{b} \sin pt, \quad \dots\dots(2.1)$$

where  $p = 2\pi \times$  frequency ( $\nu$ ),  $m$  and  $n$  are integers, and  $w_0$  is a constant. Substitution of (2.1) in (1.5) shows that the boundary conditions are satisfied, and substitution of (2.1) in the differential equation (1.3) leads directly to

$$\nu_s = \frac{\pi}{2a^2b^2} \left\{ \frac{1}{\rho h} [D_1 m^4 b^4 + D_2 n^4 a^4 + 2D_3 m^2 n^2 a^2 b^2] \right\}^{\frac{1}{2}}, \quad \dots\dots(2.2)$$

where the suffix  $s$  indicates supported edges.

The fundamental is given by  $m = n = 1$ , and the overtones by higher values of  $m$  and  $n$ .

In view of the complexity of the problem involved in a complete solution, the fundamental frequency for clamped edges has been derived by the Rayleigh method (see e.g. Timoshenko, 1937, § 16), supplemented to some extent by the use of the more accurate Ritz modification. For comparison both with the exact solution (2.2) and with the results for clamped edges, the Rayleigh and Ritz methods have also been applied to the case of simply supported edges.

The Rayleigh method consists in working out the potential energy  $V$  and the kinetic energy  $T$  from the equation

$$w = f(x, y)g(t), \quad \dots\dots(2.3)$$

which expresses the deflection  $w$  as a function of time  $t$  and of position on the plate. If the system is conservative, then

$$V_{\max} = T_{\max}, \quad \dots\dots(2.4)$$

and the frequency of vibration is found from this condition.

The virtue of the Rayleigh method is that in general it is possible to use an approximate expression of  $f(x, y)$  in (2.3) and still obtain estimates of the frequency sufficiently accurate for all practical purposes. In the present instance, the simplest algebraic expressions consistent with the boundary conditions have been chosen to represent  $f(x, y)$ . Assuming a sinusoidal vibration, this leads to

$$w = K_c x^2 y^2 (a-x)^2 (b-y)^2 \sin pt, \quad \dots\dots(2.5)$$

for clamped edges, and to

$$w = K_s xy(a-x)(b-y)(a^2 + ax - x^2)(b^2 + by - y^2) \sin pt, \quad \dots\dots(2.6)$$

for supported edges, where  $K_c$  and  $K_s$  are constants, the suffix indicating the boundary conditions. It should be noted that, although (2.5) and (2.6) satisfy the boundary conditions, they are not solutions of (1.3).

The potential energy can now be found for clamped edges by inserting  $w$ , as given by (2.5), in (1.6) :

$$V_c = \frac{a^5 b^5 K_c^2}{1575} \left[ D_1 b^4 + D_2 a^4 + \frac{4}{7} D_3 a^2 b^2 \right] \sin^2 pt, \quad \dots\dots (2.7)$$

and for supporting edges by inserting (2.6) in (1.6) :

$$V_s = \frac{62 a^5 b^5 K_s^2}{525} \left[ D_1 b^4 + D_2 a^4 + \frac{867}{434} D_3 a^2 b^2 \right] \sin^2 pt. \quad \dots\dots (2.8)$$

The kinetic energy is given similarly for clamped edges by (2.5) and (1.7) as

$$T_c = \frac{\rho h a^9 b^9 K_c^2 p^2 \cos^2 pt}{793800}, \quad \dots\dots (2.9)$$

and for supported edges by (2.6) and (1.7) as

$$T_s = \frac{961 \rho h a^9 b^9 K_s^2 p^2 \cos^2 pt}{793800}. \quad \dots\dots (2.10)$$

In each case the potential energy can be written  $V = MK^2 \sin^2 pt$  and the kinetic energy  $T = NK^2 p^2 \cos^2 pt$ . The maximum  $V$  occurs when  $\sin^2 pt = 1$  and the maximum  $T$  when  $\cos^2 pt = 1$ . Hence from condition (2.4),  $p^2 (= 4\pi^2 \nu^2) = M/N$ . Thus from equations (2.7) and (2.9)

$$\nu_c = \frac{1}{\pi a^2 b^2} \left\{ \frac{126}{\rho h} \left[ D_1 b^4 + D_2 a^4 + \frac{4}{7} D_3 a^2 b^2 \right] \right\}^{\frac{1}{2}}, \quad \dots\dots (2.11)$$

and from (2.8) and (2.10)

$$\nu_s = \frac{1}{\pi a^2 b^2} \left\{ \frac{756}{31 \rho h} \left[ D_1 b^4 + D_2 a^4 + \frac{867}{434} D_3 a^2 b^2 \right] \right\}^{\frac{1}{2}}. \quad \dots\dots (2.12)$$

Comparison of equation (2.12) with the accurate solution (2.2), putting  $m=n=1$ , shows that the form of the equations is identical, and further, the numerical coefficients are very close in the two cases. The coefficient outside the brackets in the accurate equation (2.2) is  $\pi/2 = 1.5708$ , while the corresponding coefficient in (2.12) is  $\pi^{-1} \sqrt{(756/31)} = 1.5719$ ; the coefficient of the term in  $D_3 a^2 b^2$  is 2 in equation (2.2) and  $867/434 (= 1.998)$  in equation (2.12).

In order to obtain an estimate of the degree of approximation involved in the clamped-edge solution (2.11), the Ritz modification of the Rayleigh method has been applied to the present problem. The procedure, with an example on the one-dimensional case of the vibrating string, is given in Timoshenko's book (1937, § 62). The application of the method to the two-dimensional case of the vibrating anisotropic plate does not present any special difficulties, although it leads to somewhat laborious algebra and arithmetic. For the above reasons, only the final results, and such description of the process as is required for their presentation, will be given here.

The forms assumed for  $w$  are generalizations of (2.5) and (2.6) :

(1) Clamped edges,  $w = X^2 Y^2 (K_1 + K_2 XY) \sin pt$  ;

(2) Supported edges,  $w = XY(a^2 + ax - x^2)(b^2 + by - y^2)(K_1 + K_2 XY) \sin pt$ ,  
where  $X = x(a - x)$ ,  $Y = y(b - y)$ .

If  $K_2 = 0$ , the above equations reduce respectively to (2.5) and (2.6). An essential feature of the Ritz method is that the values of  $K_1$  and  $K_2$  are adjusted at one stage in the process so as to make the frequency a minimum. With two constants, this leads to a quadratic in the frequency, one root of which gives a more accurate estimate of the fundamental frequency than that given by the Rayleigh method.

For the purpose of comparing the various estimates, it is convenient to confine attention to square plates, and, in the case of wood and plywood, to particular values of the elastic constants. For square plates, equations (2.2), (2.11) and (2.12) are of the form

$$\nu = c_1 / a^2 \sqrt{\rho h}. \quad \dots\dots (2.13)$$

Values of the constant  $c_1$  have been calculated by the Ritz method for plates of birch 5-ply and birch veneer having the following "flexural rigidities"  $D$  (c.g.s. units ; values based on elastic constants given in table 2 below).

	$D_1$	$D_2$	$D_3$
Birch 5-ply	$0.191 \times 10^{10}$	$0.071 \times 10^{10}$	$0.044 \times 10^{10}$
Birch veneer	$2.97 \times 10^8$	$0.21 \times 10^8$	$0.69 \times 10^8$

For an isotropic solid  $D_1 = D_2 = D_3$ , and it is therefore possible, by introducing this condition, to reduce any of the equations so far given to the isotropic case. The exact value of  $c_1$  for a square isotropic plate with supported edges is known (Timoshenko, 1937, equation 214) to be  $\pi\sqrt{D_1}$ , where  $D_1 = Eh^3/12(1 - \sigma^2)$ , and

Table 1. Calculated values of  $c_1$  in equation (2.13)  
(Square plates)

Method	Clamped edges			Supported edges		
	Isotropic	Birch		Isotropic	Birch	
		5-ply	Veneer		5-ply	Veneer
Rayleigh	$5.730 \sqrt{D_1}$	$1.914 \times 10^5$	$0.6755 \times 10^5$	$3.1429 \sqrt{D_1}$	$0.9300 \times 10^5$	$0.3357 \times 10^5$
Ritz	$5.729 \sqrt{D_1}$	$1.912 \times 10^5$	$0.6750 \times 10^5$	$3.1420 \sqrt{D_1}$	$0.9294 \times 10^5$	$0.3355 \times 10^5$
Exact	$5.727 \sqrt{D_1}$	—	—	$3.1416 \sqrt{D_1}$	$0.9293 \times 10^5$	$0.3354 \times 10^5$

Tomotika (1936) has given an estimate of  $c_1$  for a square plate with clamped edges which, though not strictly exact, gives a highly accurate lower limit. The various estimates for  $c_1$  are collected in table 1.

Even the largest difference in the above table is only just greater than 0.1%, and it can be concluded that the fundamental frequencies estimated by the

Rayleigh method are mathematically sufficiently accurate for the purpose of comparing theoretical with observed frequencies. The Rayleigh equations (2.11) and (2.12) have, therefore, been used in all subsequent calculations.

### § 3. EXPERIMENTAL

The general features of the method used to determine the frequencies can be seen from figures 1, 2 and 3. The wood or plywood plate was held in a suitable frame and two small iron plates A and C (figure 1) were attached by means of soft wax, one (A) at the centre of the test plate, and the other (C) a convenient distance away. A small iron-cored solenoid (B), fed by alternating current from a beat-frequency oscillator, was placed near to plate A, while a telephone receiver, stripped of its diaphragm and case, was placed so that the magnets were close to plate C. Any currents induced in the coils of the telephone were fed to a cathode-ray oscillograph, and the experiment consisted in varying the frequency of the driving current supplied to B until the response, as indicated by the oscillograph, was a maximum. The telephone receiver D was connected to the vertical plates of the oscillograph, and the driving current from the oscillator connected to the horizontal plates, in parallel with the coil B. In this way, a

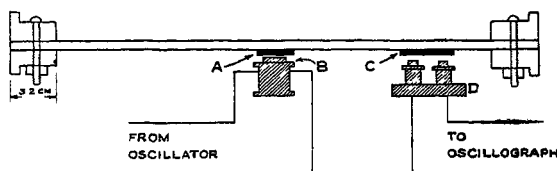


Figure 1. Experimental arrangement

Lissajous figure was obtained on the oscillograph screen, and it was found that, with the present experimental arrangement, the plates tended to respond to integral submultiples of the resonant frequency, in agreement with results, so far unpublished, on wooden strips. The most powerful response in all cases occurred when the frequency of the driving current was one-half the true resonant frequency, as is shown by the fact that the Lissajous figure indicated two vibrations of the plate for each cycle of the forcing current. The results given in table 2 are all based on this response mode.

The apparatus can, of course, be used to measure overtones, and a number of observations were actually made of the frequencies at which these occurred. Owing to certain difficulties, mainly theoretical, a satisfactory interpretation of these measurements is not available at present, and they will not be discussed further.

The frames for holding the plates were made of wood and are shown in figures 1, 2 and 3. The frame for clamped edges (general view, figure 2; cross-section, figure 1) consisted of two halves bolted together, with the plate sandwiched between them. The frame for supported edges (figure 3) consisted of four separate grooved members held together by brass bolts and wing nuts, with the edges of the plate at the base of the grooves, as shown in the section diagram, figure 3 (b).

For convenience of lining up and adjustment, the apparatus was assembled on an optical-bench base. The frames were held at opposite corners by ordinary laboratory clamps attached to vertical rods; the solenoid B and telephone receiver D were also mounted on rods, all of which were held in optical-bench stands.

The plates were originally cut to 45.8 cm. squares, and were progressively reduced in size in order to provide measurements over a range of lateral dimensions. It can be seen from equations (2.11) and (2.12) that if  $D_1$  and  $D_2$  differ,

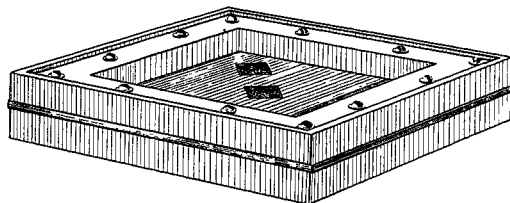


Figure 2. Clamped edge frame.

the frequency of an oblong plate of given dimensions depends on whether the direction of greater flexural rigidity coincides with the longer or shorter side of the plate, and provision was made for the testing of plates fulfilling both of these conditions. For example, two 45.8 × 45.8 cm. plates of obeche veneer were originally available (table 2). The first reduction in size was accomplished on plate 1 by shortening to 30.6 cm. the side  $a$ , lying parallel to the greater Young's modulus, and on plate 2 by shortening to the same length the side  $b$ , lying parallel

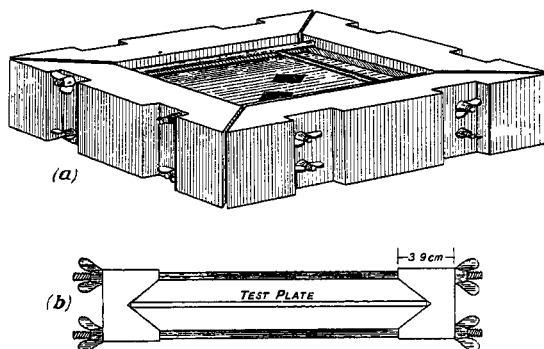


Figure 3. Supported edge frame.  
(a) General view; (b) cross-section.

to the smaller Young's modulus. On the second reduction in size, side  $b$  on plate 1 and side  $a$  on plate 2 were shortened to 30.6 cm., thus giving square plates again. This procedure was repeated once more, finally leading to the smallest size of plate, 20.4 × 20.4 cm. The dimensions given refer to the supported-edge condition; the clamped dimensions are smaller owing to the overlap of the frames (see figures 1 and 2).

Young's moduli in bending ( $E$ ), and rigidity modulus ( $G$ ), on which, by equations (1.2), the "flexural rigidities" depend, were determined respectively



Table 2. Experimental values of elastic constants, dimensions and fundamental frequencies

Veneers										Plywoods					
Obeche			Gaboona			Beech				Birch		Birch 3-ply		Opepe 3-ply	Douglas fir 3-ply
(1)	(2)	(1)	(2)	(3)	(1)	(2)	(3)	(1)	(2)	Birch 5-ply		(1)	(2)		
(1) Elastic constants															
$E_1$	6.9	7.4	7.8	7.9	8.7	13.3	13.3	13.3	11.7	9.3	12.0	12.4	9.3	8.4	
$E_2$	0.17	0.05	0.30	0.19	0.14	0.55	0.54	0.82	0.82	3.45	1.19	1.21	0.80	1.08	
$E_1 \rho_{21}$	0.17	0.17	0.19	0.19	0.22	0.33	0.33	0.37	0.37	0.37	0.37	0.37	0.25	0.25	
$G_{12}$	0.30	0.34	0.58	0.45	0.41	0.85	0.86	1.19	0.90	0.90	0.88	0.93	0.54	0.90	
$h$ (cm.)	0.291	0.323	0.318	0.310	0.315	0.309	0.309	0.311	0.311	0.626	0.532	0.525	0.479	0.415	
$\rho$ (gm./cc.)	0.330	0.390	0.400	0.399	0.393	0.670	0.659	0.719	0.719	0.690	0.716	0.711	0.774	0.533	
(2) Observed fundamental frequencies (cycles/sec.). Clamped edges															
$a=b=39.3$ cm.	67	82	76	76	78	89	82	—	—	160	140	148	—	—	
$a=24.2, b=39.3$	172	—	192	—	—	—	182	—	—	—	—	254	—	—	
$a=39.3, b=24.2$	—	88	—	96	92	95	—	96	96	254	197	—	155	162	
$a=b=24.2$ cm.	189	191	202	156	202	200	225	212	212	392	320	326	270	278	
$a=14.0, b=24.2$	506	—	496	—	—	—	440	—	—	—	—	706	—	—	
$a=24.2, b=14.0$	—	201	—	229	224	241	—	248	248	650	486	—	375	382	
$a=b=14.0$ cm.	444	502	556	510	524	530	514	544	544	980	830	850	654	618	
(3) Observed fundamental frequencies (cycles/sec.). Supported edges															
$a=b=45.8$ cm.	35	39	40	34	38	41	43	—	—	73	67	61	—	—	
$a=30.6, b=45.8$	92	—	94	—	—	—	95	—	—	—	—	152	—	—	
$a=45.8, b=30.6$	—	60	—	68	50	53	—	52	52	150	82	—	77	90	
$a=b=30.6$ cm.	81	114	105	88	92	84	94	108	108	187	190	180	120	137	
$a=20.4, b=30.6$	186	—	181	—	—	—	166	—	—	—	—	320	—	—	
$a=30.6, b=20.4$	—	94	—	109	92	106	—	123	123	281	200	—	167	168	
$a=b=20.4$ cm.	184	190	218	182	182	186	191	228	228	420	390	374	296	278	

by flexural and torsional vibration experiments (Hearmon and Barkas, 1941) on approximately 2.5-cm. wide strips of the material cut parallel to and near the sides of the largest plates. The Poisson's ratios ( $\sigma$ ) were not measured, but were obtained from published values of  $\sigma$  for the appropriate solid wood. In some cases, no relevant measurements could be found, and it was then assumed that the Poisson's ratio for solid wood,  $\frac{\text{contraction along the grain}}{\text{extension across the grain}}$  for tension across the grain, had the value 0.025. As in much work on wood and plywood, the contribution of the terms involving the Poisson's ratios is small, and the exact values adopted are not very important.

#### § 4. RESULTS AND DISCUSSION

The complete experimental results are given in table 2; the side  $a$  is taken as parallel with the direction of  $E_1$  and  $b$  with  $E_2$ , where  $E_1 > E_2$ .

In order to compare the observed and theoretical frequencies, it is convenient to express the equations for the latter in terms of elastic constants, rather than flexural rigidities, by substituting equations (1.2) in (2.11) and (2.12). Thus,

$$\nu_c = \frac{1.04h}{a^2\sqrt{\rho}} \left[ E_1 + \left(\frac{a}{b}\right)^4 E_2 + \left(\frac{a}{b}\right)^2 (0.57E_1\sigma_{21} + 1.13G_{12}) \right]^{\frac{1}{2}} \dots (4.1)$$

and

$$\nu_s = \frac{0.456h}{a^2\sqrt{\rho}} \left[ E_1 + \left(\frac{a}{b}\right)^4 E_2 + \left(\frac{a}{b}\right)^2 (2.00E_1\sigma_{21} + 3.96G_{12}) \right]^{\frac{1}{2}}, \dots (4.2)$$

where  $\lambda$  has been put equal to 0.99, and the numerical coefficients are given to three significant figures.

The observed frequencies are plotted against those calculated from (4.1) and (4.2) in figures 4 and 5. The lines in these figures are not necessarily the "best" fit, but are drawn through the origin with slope determined by the average value of the ratio (observed frequency/calculated frequency) for all the observations. Numerically, this average is 0.772 for clamped edges and 1.238 for supported edges. Thus, the calculated frequencies with edges clamped are consistently higher than the observed frequencies, while the reverse is true for the supported edges. This suggests that the actual conditions at the edges of the plates are always intermediate between the conditions appropriate to strictly clamped and supported edges (equations (1.4) and (1.5)). The difficulty of realizing experimentally the exact boundary conditions assumed in the theoretical treatment of this type of problem is well known, and has been encountered, for example, in buckling tests of plywood panels in shear (Norris, Voss and Palma, 1945).

Ideally, of course, the points in figures 4 and 5 should lie on a line passing through the origin, and having a slope of  $45^\circ$ ; the general tendency of the points to depart from this line is a measure of the effect just discussed. In addition, there is also a certain amount of random scatter, which is partly accounted for by casual experimental errors in the frequency measurements, or by variation in the material between the test plates and the strips used in the determination of elastic constants.

Superimposed on all these effects, however, there is definite indication that with clamped edges (figure 4) the best line through the points is curved, and not straight; the curvature is such that the ratio ( $\nu$  observed/ $\nu$  calculated) becomes smaller at higher frequencies. The physical interpretation of this result is that the frame used for clamped edges becomes less effective with thicker plates and smaller lateral dimensions, and under these conditions departures from the ideal clamped-edge conditions tend to be higher.

In order to obtain further information on this effect, a mild steel frame was made to hold the smallest square plates in the clamped-edge condition. This frame was of the same dimensions as the corresponding wooden frame; the two halves, however, were held together by twelve  $\frac{1}{4}$ -in. bolts instead of the  $\frac{1}{8}$ -in. size used with the wooden frame. The observed frequencies in the steel and wooden frames and the theoretical frequencies (equation (4.1)) are given in table 3.

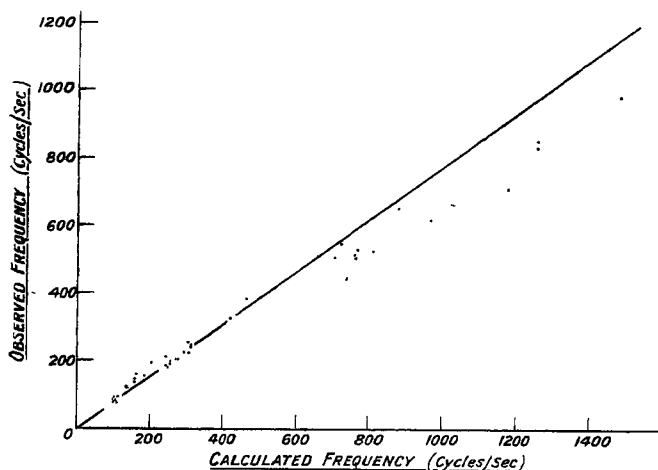


Figure 4 All results, clamped edges.

In each case the frequency is higher in the steel frame than in the wooden frame, and is, therefore, closer to the calculated frequency. The average ratio (observed frequency/calculated frequency) is 0.67 for the wooden frame and 0.83 for the mild-steel frame. These results confirm that a considerable part at least of the discrepancy between observed and calculated frequencies can be attributed to the conditions at the edges of the plates.

With the exception of the opepe 3-ply, the observed frequencies in the steel frame are lower than those calculated. This suggests that, even in the steel frame, the restraint at the edges is not sufficient to realize fully the ideal clamped-edge conditions.

Inspection of figure 5 (simply supported edges) does not reveal any marked tendency to curvature, though statistical analysis (see table 4) shows that there is in fact a slight tendency to curvature such that the ratio (observed frequency/calculated frequency) *increases* somewhat as the frequency rises. It is rather surprising that the supported-edge frame should prove more

Table 3. Frequencies in cycles/sec. Edges clamped ;  $a = b = 14.0$  cm.

Material	Obeche		Gaboon			Beech		Birch	Birch 5-ply	Birch 3-ply		Opepe 3-ply	Douglas fir 3-ply
	(1)	(2)	(1)	(2)	(3)	(1)	(2)			(1)	(2)		
Frequency (wooden frame)	444	502	556	510	524	530	514	544	980	830	850	654	618
Frequency (steel frame)	514	585	642	593	613	637	628	647	1220	1110	1110	960	770
Frequency (calculated)	740	770	800	770	810	780	790	730	1490	1260	1270	950	980

satisfactory in this respect than the clamped-edge frame, because the former has quite apparent defects. There is a small area near each corner which is unrestrained, but, perhaps more important, the degree to which the wing nuts holding the frame together (figure 3) are tightened is a matter for personal judgment in obtaining a sufficiently firm fixing of the test plate without applying appreciable compressions in its plane. Nevertheless, the experimental results indicate that, although the conditions at the edges do not constitute true simple support, they are to a first approximation independent of the dimensions of the plate.

In view of the rough proportionality between elastic constants and density of timber, it is possible to derive certain empirical relations which enable the frequencies to be estimated even if the elastic constants and densities are not

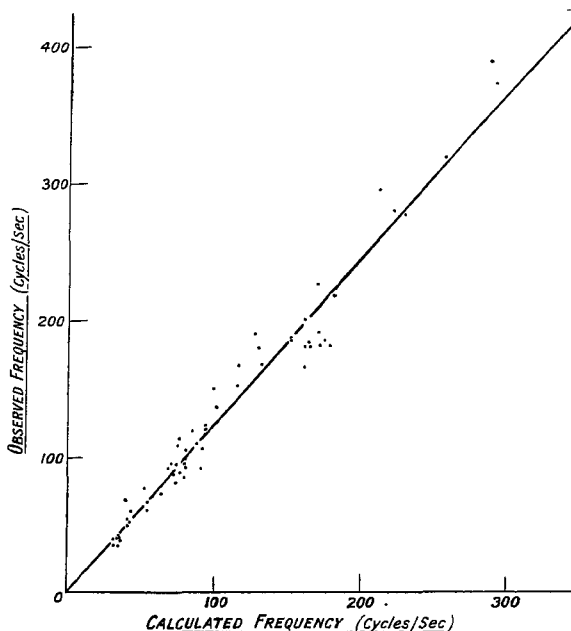


Figure 5. All results, supported edges.

known. If it is assumed that elastic constants are exactly proportional to density, then equations (4.1) and (4.2) take the form

$$\nu = c_2 h / a^2, \quad \dots \dots (4.3)$$

where  $c_2$  is a numerical factor which depends only on the edge conditions and on the ratio  $a/b$ .

Two related consequences follow from (4.3) :

(1) For given edge conditions, and given ratios  $a/b$  and  $h/a^2$ , the frequency should be constant irrespective of the values of elastic constants and density. Examination of the experimental results for the veneers in table 2, all of which have a thickness of about 0.3 cm., shows that this prediction is approximately verified.

(2) For given edge conditions, and a given value of  $a/b$ , a plot of  $\nu$  against  $h/a^2$  should give a straight line passing through the origin. The theoretical frequencies for square plates are plotted on this basis in figures 6 and 7, and it

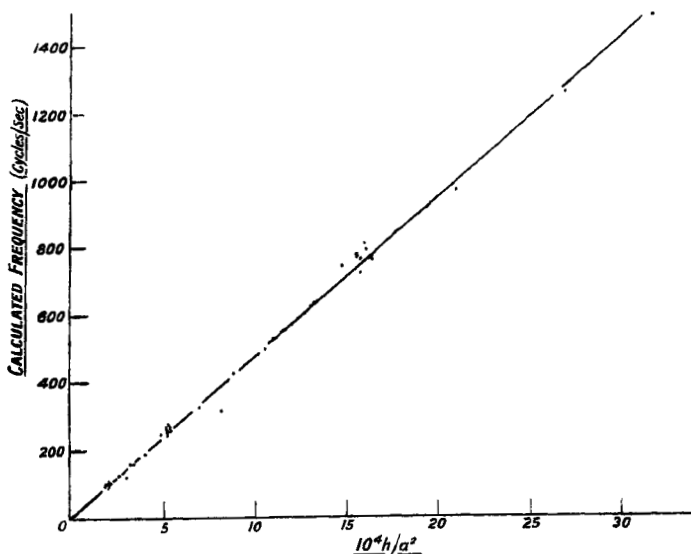


Figure 6. Square plates, clamped edges.

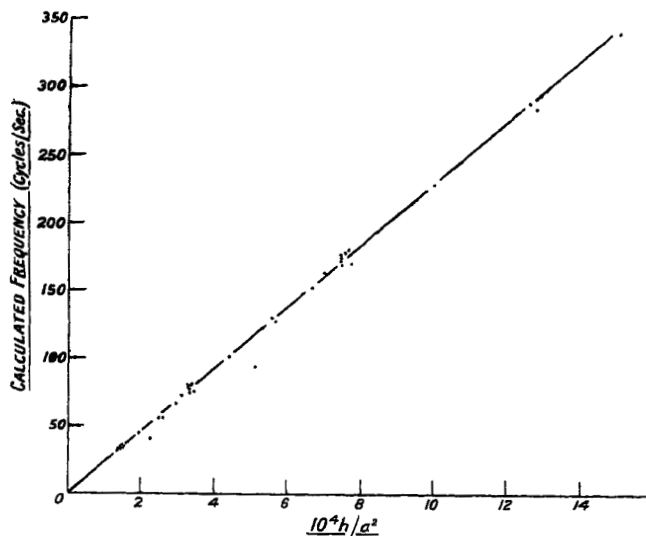


Figure 7. Square plates, supported edges.

will be seen that, apart from three exceptionally low frequencies in each figure, the points lie very close to the lines

$$\nu_c = 47 \times 10^4 h/a^2 \text{ (clamped edges),} \quad \dots\dots(4.4)$$

$$\nu_s = 23 \times 10^4 h/a^2 \text{ (supported edges).} \quad \dots\dots(4.5)$$

The exceptionally low frequencies all refer to the opepe 3-ply, and serve as a reminder that this method of estimating frequencies must necessarily give results somewhat in error in those cases where the assumed proportionality between elastic constants and density does not hold.

The theoretical frequencies for oblong plates have been analysed in the same way and have given the following equations :

Clamped edges :

$$\begin{aligned} a/b &= 2/3, & \nu_c &\approx 45 \times 10^4 h/a^2; \\ a/b &= 3/2, & \nu_c &\approx 55 \times 10^4 h/a^2. \end{aligned}$$

Supported edges :

$$\begin{aligned} a/b &= 2/3, & \nu_s &\approx 21 \times 10^4 h/a^2; \\ a/b &= 3/2, & \nu_s &\approx 29 \times 10^4 h/a^2. \end{aligned}$$

It will be remembered that  $a$  is the length of side parallel to the direction of greatest Young's modulus. The scatter of the points for  $a/b = 2/3$  is greater than that shown for square plates in figures 6 and 7, and the uncertainty in the predicted frequency is therefore greater in this case.

The experimental results for square plates (table 2) have been analysed statistically on the above basis, both as a whole and in groups corresponding with the different sizes of plate. The regression equations for predicting the experimentally observed frequencies in terms of  $y (= 10^4 h/a^2)$  are summarized in table 4.

Table 4. Summary of regression equations  
( $\nu$  = observed frequency,  $y = 10^4 h/a^2$ )

Clamped edges		Supported edges	
$a=b=39.3$ cm.	$\nu=42.9y-7.3$	$a=b=45.8$ cm.	$\nu=23.6y+3.8$
$a=b=24.2$ cm.	$\nu=34.4y+14.9$	$a=b=30.6$ cm.	$\nu=30.7y-6.1$
$a=b=14.0$ cm.	$\nu=27.7y+70.2$	$a=b=20.4$ cm.	$\nu=31.8y-44.0$
All results	$\nu=29.3y+38.7$	All results	$\nu=28.3y-2.9$

For the largest sizes, the equations are not very different from (4.4) and (4.5), which are derived from the theoretical frequencies. With clamped edges there is a noticeable decrease in the slope of the lines and an increase in the intercept on the  $y$  axis with decreasing size of plate. These effects are reflections of the tendency to curvature already discussed in connection with figure 4. The supported-edge results show a slight tendency to curvature in the opposite direction when analysed in this way, although, as already mentioned, this tendency is not obvious on inspection of figure 5. In other words, the edge conditions in the frames tend to approach each other at the higher frequencies, and there are indications that at the highest frequencies the "clamped"-edge frame may even impose less restraint at the edges than the "supported"-edge frame.

#### ACKNOWLEDGMENTS

The work described above was carried out in the Physics Section, Forest Products Research Laboratory, as part of the programme of the Forest Products

Research Board, and publication is by permission of the Department of Scientific and Industrial Research. The statistical analyses summarized in table 4 were carried out under the direction of Miss C. B. Pettifor, B.Sc.

## REFERENCES

- GOLAND, M., 1942. Curtiss-Wright Corporation, Airplane Division, *Research Report*, 5 S, 13.  
 HEARMON, R. F. S. and BARKAS, W. W., 1941. *Proc. Phys. Soc.* 53, 674.  
 MARCH, H. W., 1936. *Physics*, 7, 32.  
 MARCH, H. W., 1942. U.S. Dept. Agric. Forest Prod. Lab., Madison, Mimeo. 1312.  
 NORRIS, C. B., VOSS, A. W. and PALMA, J., 1945. U.S. Dept. Agric. Forest Prod. Lab., Madison, Mimeo. 1316 H.  
 TIMOSHENKO, S., 1937. *Vibration Problems in Engineering* (New York: Van Nostrand).  
 TIMOSHENKO, S., 1940. *The Theory of Plates and Shells* (New York: McGraw-Hill).  
 TOMOTIKA, S., 1936. *Phil. Mag.* 21, 745.

## THE OPTICAL SINE-CONDITION

BY H. H. HOPKINS,

W. Watson and Sons, Barnet, Herts

MS. received 20 September 1945

**ABSTRACT.** The Sine-Condition is formulated on the basis of optical path differences, leading to an expression which is valid in the presence of spherical aberration. It is shown to contain results obtained previously by means of a "ray-intersection" analysis. The "next terms" are estimated and serve as an approximate measure of the error involved; or, alternatively, as an indication of the size of field over which the sine-condition is a valid measure of off-axis aberration.

IT is well known that fulfilment of the so-called *Sine-Condition* by an optical system ensures freedom from the aberration of coma for objects that are but a small angular distance from the axis. Because of this fact, the sine-condition has been used extensively by lens designers as a check on the off-axis performance of both telescope and microscope objectives. There are, however, respects in which this usage has been unsatisfactory.

In the first place the condition is a valid measure of off-axis aberration only when the angular distance off-axis of the object point is so small that its square can be neglected. There is an uncertainty in the size of field over which this approximation is permissible, given a required order of accuracy in the result. Secondly, the physical meaning which can be attached to the violation of the condition is—in my experience—generally not appreciated. The permitted departures from exact fulfilment of the sine-condition are consequently either wholly arbitrary or based on experience of "what works". It is true that Conrady (*Applied Optics and Optical Design*, vol. i, p. 393) gave a "Rayleigh tolerance" for coma, but this was simply quoted without proof.

In what follows, an account of the imagery of off-axis object points is given which leads to a simple interpretation of departures from the sine-condition